LC3-II, lipidated). LC3-II is closely associated with the preautophagosomal and autophagosomal membrane.[20,21] Many studies have used LC3 to investigate the activity of autophagy in various disease models.[15,17] Previous research demonstrated that the expression of LC3 increased at lesion sites after traumatic brain injury and cerebral ischemia.[16,22–27] These studies suggested that the autophagic activity was increased in damaged neural tissue of brain.

In many previous studies, an anatomic analysis using electron microscopy has been used to determine the activity of autophagy.[15,17] The anatomic formation of autophagic vacuoles is morphologic evidence of autophagy.[20,21] Recent studies have demonstrated an increased formation of autophagic vacuoles to be observed in lesions of ischemic and traumatic brain injury.[22,24–27] However, there has so far been no study that investigated the anatomic formation of autophagic vacuoles in the lesion after spinal cord injury (SCI).

To date, previous studies have mainly focused on apoptotic process but not autophagic activity as mechanism of neural tissue damage after SCI. Only our previous study demonstrated that a promoter of autophagy, Beclin 1, increased in the injured spinal cord.[28] However, recent studies clarified that the autophagic activity is regulated by not only Beclin 1 but also other molecular factors including mTOR, Bcl-family, DRAM, p53, and NF-κB. The activity of autophagy is suppressed by mTOR, Bcl-family, p53, and NF-κB.[12,29] The Beclin 1 expression does not directly indicate the induction of autophagy. Therefore, it is necessary to investigate the changes in the LC3 expression and the anatomic formation of autophagic vacuoles to provide the evidence of autophagy activation in the damaged neural tissue after SCI.

This study investigated the activation of autophagy after SCI, using a spinal cord hemisection model in mice. The changes in LC3 protein expression were examined by immunohistochemistry and Western blot analysis. In addition, electron microscopic analysis was performed to examine the anatomic formation of autophagy and autophagic cell death in the injured spinal cord.

MATERIALS AND METHODS

Animals and Surgical Procedures

All experimental procedures were approved by the Institutional Animal Care and Use Committee of Tohoku University. A total of 40 adult female C57BL/6J mice (10–12 weeks old; Charles River, Japan Inc., Yokohama, Japan) were used in this study. Three or five animals were used in each experimental group at each time point. The mice were anesthetized with 1.25% halothane in an oxygen/nitrous oxide (30/70%) gas mixture. During surgery, the rectal temperature was monitored and maintained at 37.0 ± 0.5°C by a heating pad. The skin above the thoracic vertebrae was shaved and cleaned in an antiseptic manner. A 15-mm midline skin incision was made. The laminae of T9–T11 were exposed. A laminectomy was performed at T10, and the dura mater was exposed. The spinal cord was hemitransected with a sharp scalpel on the right side only.[28,30,31] The muscles and skin were closed in layers. No active motion of the hindlimb on the injured side was observed in any of the animals after hemisection. In addition, no obvious recovery of the hindlimb motion occurred during this study. The mice with a compromised bladder function (a rare complication) were treated with manual bladder expression twice a day until reflex bladder emptying was established. The sham-operated animals received the same surgical procedures, but no hemisection was applied to the spinal cord.

Tissue Preparation

At different time points (4 hours, 24 hours, 3 days, 7 days, and 21 days) after a hemisection and immediately after the sham operation, the mice were overdosed by an intraperitoneal injection of 100 mg/kg sodium pentobarbital. The mice were transcardially perfused with normal saline, followed by 4% paraformaldehyde in 0.1 M phosphate-buffered saline (PBS), pH 7.4. For immunohistochemical staining, the spinal cord segments (8 mm in length) centered at the injured site were collected, postfixed in the same fixative overnight at 4°C, and embedded in paraffin. Serial 7-μm transverse and horizontal sections around the injured site were mounted on slides. A total of 13 sequential transverse sections at 250-μm intervals were collected, spanning a 3000-μm length in the spinal cord centered at the epicenter. The sections were used for immunohistochemical staining as described later.

Immunohistochemical Staining of LC3

Immunohistochemical staining of LC3 was performed using the sections at each observation point to investigate alterations of the expression of LC3 in the spinal cord after hemisection. The sections were deparaffinized and rehydrated and then were washed in PBS for 10 minutes, followed by washing with PBS containing 0.3% Tween for 10 minutes, and blocked with 3% milk and 5% fetal bovine serum in 0.01 M PBS for 2 hours. The sections were incubated with rabbit anti-LC3 antibodies (1:100; Marine Biological Laboratory, Woods Hole, MA) diluted in PBS overnight at 4°C. After rinsing with PBS, the sections were incubated with goat anti-rabbit IgG Alexa Fluor 594 secondary antibody (1:500; Molecular Probes, Eugene, OR) for 1 hour at room temperature. The sections were mounted with Vectashield containing DAPI to label the nuclei (Vector Laboratories, Youngstown, OH).

Counting and Calculation of LC3-Positive Cells

Each transverse section was scanned using a laser microscope (BX 51; Olympus, Tokyo, Japan) after the immunochemical staining of LC3. The LC3-positive cells, which were defined as the cells displaying punctate LC3 fluorescence dots,[16,19] were counted in the injured and the contralateral sides of the spinal cord in the transverse sections. A total of 13 sequential transverse sections at 250-μm intervals were collected, spanning a 3000-μm length in the spinal cord centered at the epicenter. The LC3-positive cells were counted in each section. The section with the maximum number of LC3-positive cells in the injured side and 250-μm rostral and caudal sections

were chosen for each animal. The sum of the numbers in the three sections was compared between the injured side, the contralateral side, and the sham group.

Western Blot Analysis of LC3

The mice were killed at 3 days after spinal cord hemisection and after sham operation, and their spinal cords were removed. The spinal cords were homogenized in lysis buffer containing 50 mmol/L Tris HCl (pH 7.6), 20 mmol/L MgCl2, 150 mmol/L NaCl, 0.5% Triton-X, 5 U/mL aprotenin, 5 g/mL leupeptin, 5 g/mL pepstatin, 1 mmol/L benzamidine, and 1 mmol/L phenylmethylsulfonyl fluoride. The debris was removed by centrifugation, and the protein levels in the lysates were determined with the aid of the Bio-Rad protein assay (Bio-Rad Laboratories, GmbH, Munich, Germany). The protein (50 g) in the lysates was separated by SDS–polyacrylamide gel electrophoresis in 15% gels and then electrophoretically transferred to a polyvinylidene difluoride membrane. The membranes were blocked for 1 hour in tris-buffered saline with Tween (0.01 M Tris HCl, pH 7.5; 0.15 M NaCl; and 0.05% Tween 20) containing 3% milk, and incubated with rabbit anti-LC3 antibody (1:500; Marine Biological Laboratories) diluted in tris-buffered saline with Tween buffer overnight at 4°C. The membranes were washed three times and incubated with secondary antibody linked to horseradish peroxidase (1:1000; Invitrogen, Carlsbad, CA) for 1 hour at room temperature. The immunoreactive bands were developed using the enhanced chemiluminescence reagent (Amersham Corp., Van Nuys, CA) and digitalized by LAS-1000 Pro (FUJIFILM, Tokyo, Japan). The band densities of LC3-II were quantified using a scanned densitometric analysis and the Image J 1.37v software program (National Institutes of Health, Maryland, MD). The quantities of the band densities were normalized by β-tubulin, and thereafter, those quantities were compared between the injured side and the sham control.

Double Staining for LC3 and Various Cell-Type Markers

To examine the expression of LC3 in a specific population of cells, the transverse sections obtained at 3 days after hemisection were double-stained for LC3 and various cell-type markers: NeuN for neurons, GFAP for astrocytes, and Olig2 for oligodendrocytes. The sections were incubated with a mixture of rabbit anti-LC3 antibody (1:100; Marine Biological Laboratories), and goat anti-Olig2 (1:100; Santa Cruz Biotechnology, Santa Cruz, CA), mouse anti-GFAP (1:50; Dako, Carpinteria, CA), or mouse anti-NeuN antibodies (1:100; Chemicon International, Temecula, CA) diluted in PBS overnight at 4°C. After rinsing with PBS, the sections were incubated with a mixture of goat anti-rabbit IgG Alexa Fluor 594 antibody (1:500; Molecular Probes), and either donkey anti-goat IgG Alexa Fluor 488 (1:500; Molecular Probes) or goat anti-mouse IgG Alexa Fluor 488 antibodies (1:500; Molecular Probes) for 1 hour at room temperature. The sections were mounted with Vectashield containing DAPI to label the nuclei (Vector Laboratories).

Electron Microscopy

At 3 days after performing the hemisection, the mice were overdosed by an intraperitoneal injection of 100 mg/kg sodium pentobarbital. The mice were transcardially perfused with normal saline, followed by 2% paraformaldehyde and 2.5% glutaraldehyde in cacodylate buffer. For electron microscopic analyses, the spinal cord segments containing the injured site were removed and postfixed in the same fixative overnight at 4°C. The spinal cords were then cut with a sharp razor blade and serial 1 mm-transverse slices around the injured site were obtained. These tissue slices were postfixed in 1% osmium tetroxide for 1 hour at 4°C, rinsed in PBS, dehydrated in a graded series of alcohol and propylene oxide, and embedded in Epon.

Blocks showing a predominantly transverse orientation of the injured spinal cords were selected from toluidine-blue-stained thick sections. Ultrathin (70 nm) sections were prepared on an ultramicrotome (Ultracut R, Leica, Heerbrugg, Switzerland) with a diamond knife and then were stained with uranyl acetate and lead citrate and viewed using an electron microscope (JEM-1010, JOEL, Tokyo, Japan).

Double Staining of LC3 and Transferase-Mediated dUTP Nick End Labeling

To identify DNA fragmentation in the cells expressing LC3, double staining of LC3 and the terminal deoxynucleotidyl transferase-mediated dUTP nick end labeling (TUNEL) was performed. Double staining was applied to the transverse sections at 3 days after hemisection, using the In Situ Cell Death Detection Kit (Roche Diagnostics, Indianapolis, IN). After immunohistochemical staining of LC3 as described earlier, the sections were washed three times in PBS. The sections were incubated in permeabilization solution (0.1% sodium citrate and 0.1% Triton X-100) for 5 minutes at room temperature and then in the TUNEL solution containing FITC-dUTP for 30 minutes at 37°C. Finally, the sections were washed in PBS and mounted for the analysis.

STATISTICAL ANALYSIS

Significant differences in the number of LC3-positive cells and in the band densities of a Western blot were analyzed using the unpaired *t* test. In all analyses, a *P* value of less than 0.05 was considered to be statistically significant.

RESULTS

Immunohistochemical Staining of LC3

Immunohistochemical staining showed that cells expressing LC3 were increased on the injured side in comparison to the contralateral side at 3 days after hemisection. The cells expressing LC3 were observed in both the gray matter and the white matter of the injured side. However, cells on the injured side did not entirely express LC3. The increase in the number of cells expressing LC3 was mainly observed within 100 μm of the rostral and caudal areas from the lesion center. In addition, the cells expressing LC3 slightly increased within 200 μm of the rostral and caudal areas. On the contralateral side,

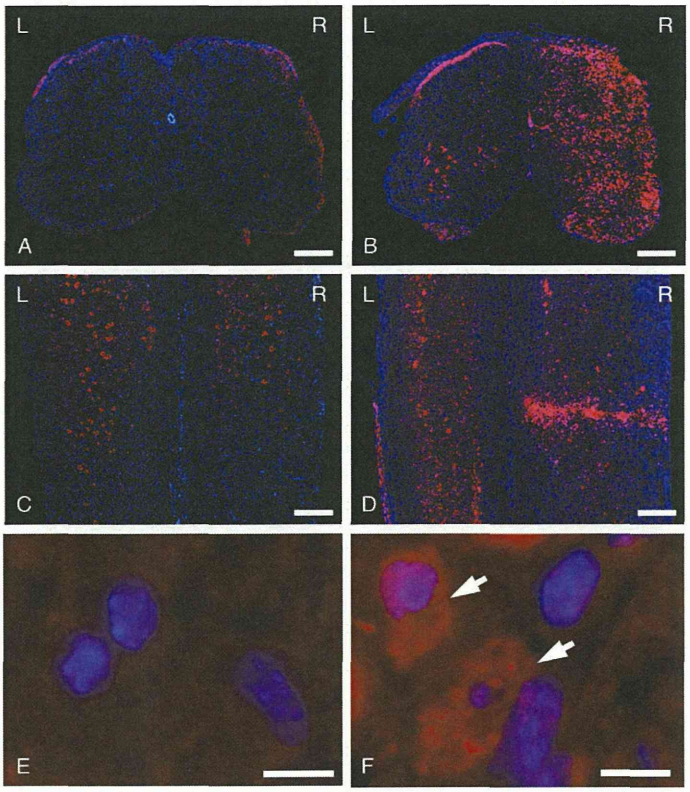

Figure 1. Immunohistochemical staining of LC3 (red) and DAPI (blue) in transverse and horizontal sections at 3 days after hemisection (**B**, **D**, **E**, **F**) and sham operation (**A**, **C**). The cells expressing LC3 were increased on the injured side (R) in comparison to the contralateral side (L) in the transverse (**B**) and horizontal (**D**) sections at 3 days after hemisection. In higher magnification, the cell expressing LC3 on the injured side displayed bright, punctate LC3 dots that were located in the cytoplasm (arrows in **F**). The cells not expressing LC3 on the contralateral side (**E**). Scale bars = 200 μm (**A**–**D**); 10 μm (**E**, **F**).

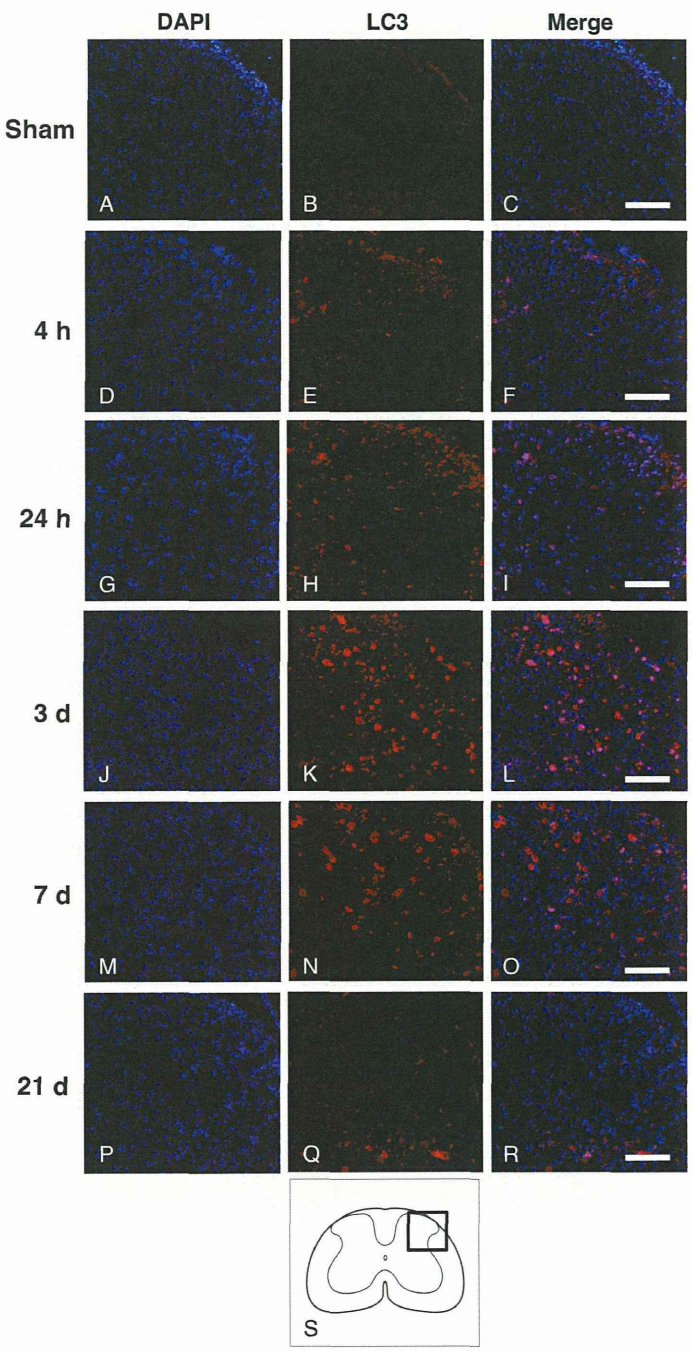

Figure 2. Immunohistochemical staining of LC3 on the injured side in transverse sections at different time points. The LC3-positive cells were increased at each time point (**D**–**R**) in comparison to the sham group (**A**–**C**). The population of the LC3-positive cells was relatively higher at 24 hours, 3 days, and 7 days (**H**, **K**, **N**) than at the other time points. Scale bar = 100 μm. The schematic drawing illustrates the location of the micrographs (**S**).

the number of cells expressing LC3 was obviously low and similar to that in the sham group (Figures 1A–D). A higher magnification on the injured side revealed the cells expressing LC3 to display bright, punctate LC3 dots that were located in the cytoplasm (Figure 1E, F). The number of cells expressing LC3 on the injured side was increased at each time point in comparison to the sham group. The population of these cells was relatively higher at 24 hours, 3 days, and 7 days than at the other time points (Figure 2).

Counting and Calculation of the LC3-Positive Cells

The number of LC3-positive cells on the injured side was significantly higher than those on the contralateral side at 3 days ($P = 0.015$). The increase of the LC3-positive cells commenced at 4 hours and lasted for at least 21 days. The maximum number of LC3-positive cells on the injured side was observed at 3 days, and it thereafter decreased at 7 days after hemisection (Figure 3).

Western Blot Analysis of LC3

The level of LC3-II protein was significantly higher in the injured side than in the sham control (Figure 4A). In the analysis of the band density, the level of LC3-II expression was 3.4 ± 0.2-fold higher in the injured side than in the sham control ($P = 0.012$; Figure 4B).

Double Staining of LC3 and Various Cell-Type Markers

Double staining of LC3 and various cell type markers revealed that the LC3-positive cells were observed in NeuN, GFAP,

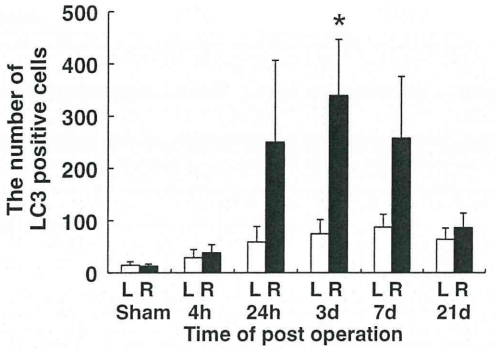

Figure 3. LC3-positive cells counted in the injured and the contralateral sides at different time points. The number of LC3-positive cells on the injured side (R) was significantly higher than those on the contralateral side (L) at 3 days ($P = 0.015$). At all time points, the number of LC3-positive cells on the injured side was higher than those on the contralateral side. The maximum number of LC3-positive cells in the injured side was observed at 3 days, and it decreased after 7 days. The values are mean ± SD. (*$P < 0.05$, n = 3 per each group).

and Olig2 labeled cells on the injured side in the transverse sections at 3 days after hemisection (Figure 5). However, these cells were not entirely LC3 positive.

Electron Microscopic Analysis

The electron microscopic analysis at 3 days after the hemisection demonstrated that the cells in contralateral side possessed bright normal nuclei, endoplasmic reticulum, Golgi apparatus, and mitochondria, which seemed not to be damaged. The formation of autophagic vacuoles was not seen in cells on the contralateral side (Figures 6A–D). In contrast, the damaged cells displayed the near-complete lysis of the organelles in the cytoplasm on the injured side. The formations of numerous autophagic vacuoles including autophagosome with double-membrane structures and multilamellar bodies were observed in the damaged cells on the injured side (Figures 6E–N). A higher magnification showed that the autophagosomes were containing membranous structures and parts of the cytoplasm (Figures 6I–N).

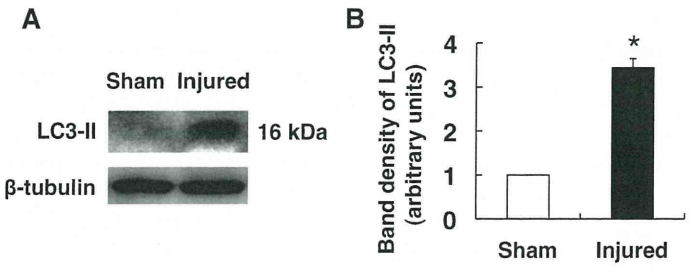

Figure 4. The expression of LC3-II protein in the injured side after hemisection and sham operation in Western blot (**A**, **B**). (**A**) The expression of LC3-II obviously increased in the injured side. (**B**) A quantitative analysis of Western blots showed that the levels of LC3-II protein on the injured side were significantly higher than that in the sham group ($P = 0.012$). The quantities of the band densities were normalized by β-tubulin. The values are mean ± SD (*$P < 0.05$, n = 5 per each group).

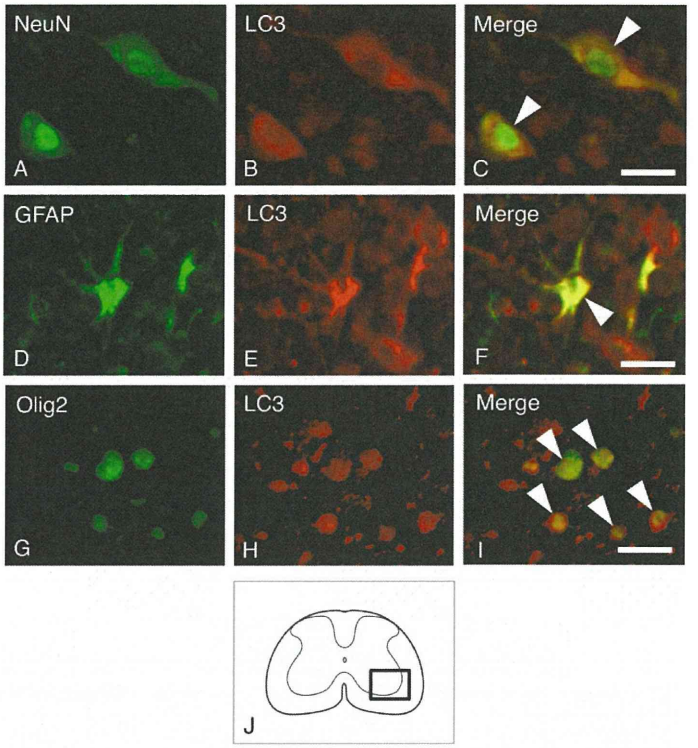

Figure 5. Double staining of LC3 (red) and cell type makers (green) on the injured side in transverse section at 3 days after hemisection (**A–I**). The LC3-positive cells were observed in the NeuN, GFAP, and Olig2-labeled cells (arrowheads in **C**, **F**, **I**). Scale bar = 20 μm. The schematic drawing illustrates the location of the micrographs (**J**).

Double Staining of LC3 and TUNEL

Double staining of LC3 and TUNEL at 3 days after hemisection showed that the number of TUNEL-positive cells as well as LC3-positive cells on the injured side obviously increased (Figures 7A–C). However, the TUNEL-positive cells were not all LC3 positive. In addition, the LC3-positive cells were not all TUNEL positive. Higher magnification revealed that the nuclei of the TUNEL-positive cells that were not LC3 positive were shrunken or fragmented, typical of apoptotic nuclei (Figures 7D–F). On the contrary, the nuclei of the TUNEL-positive cells that were found to be LC3 positive were round, as in autophagic cell death, and they were neither shrunken nor fragmented.

DISCUSSION

In this study, the number of the LC3-positive cells significantly increased at the lesion site after hemisection. An increase in the number of LC3-positive cells at the injured site was observed from 4 hours, peaked at 3 days, and then lasted for at least 21 days after injury. The LC3-positive cells were observed in neurons, astrocytes, and oligodendrocytes. A Western blot analysis demonstrated the level of LC3-II protein expression to significantly increase in the injured spinal cord. Under electron microscopy, the formation of autophagic vacuoles was obviously increased in the damaged cells. In addition, the nuclei in the TUNEL-positive cells showed that LC3 positive were round, which is consistent with autophagic cell death, and they were neither shrunken nor fragmented as observed

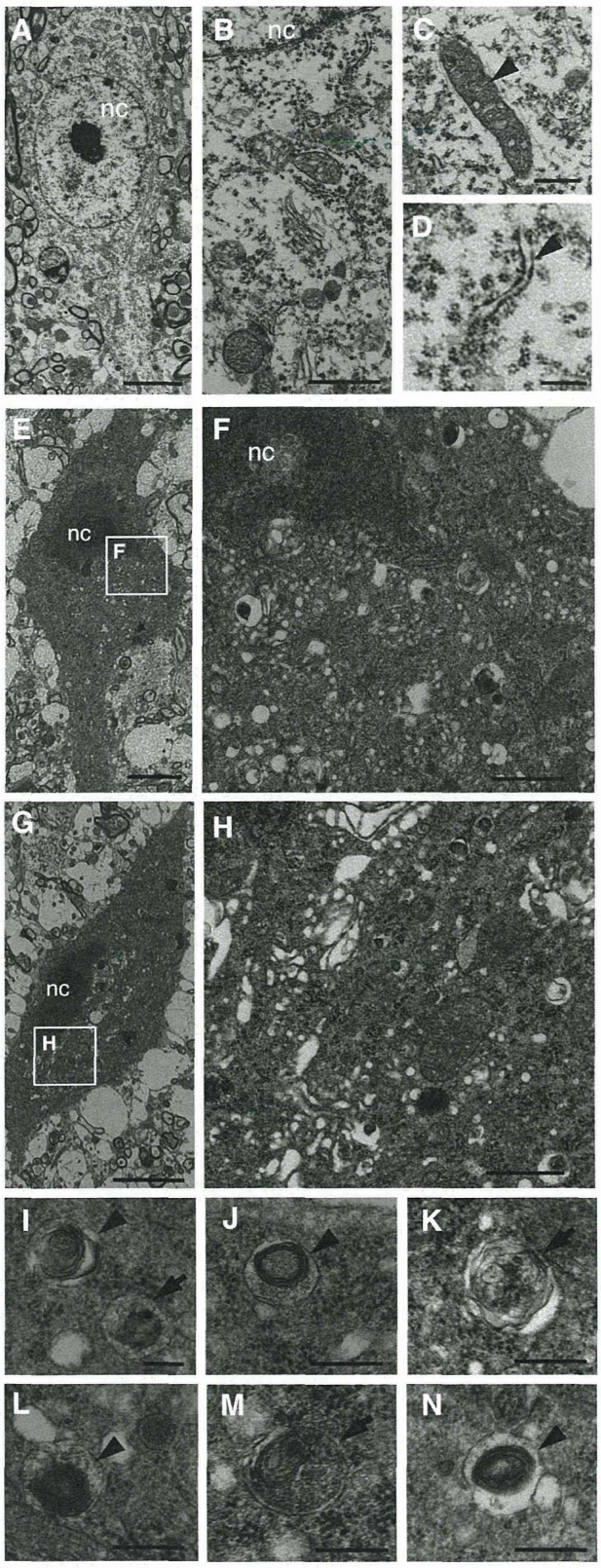

Figure 6. Electron micrographs of the neurons on the contralateral side (**A–D**) and the injured side (**E–N**) at 3 days after hemisection. The neuron in the contralateral side possessed a normal bright nucleus (nc) (**A, B**), mitochondrion (arrowhead in **C**), endoplasmic reticulum (arrowhead in **D**), which seemed not to be damaged. Autophagic vacuoles were not seen in cells on the contralateral side (**B**). In contrast, the damaged neuron on the injured side showed condensation of both the nucleus (nc) and cytoplasm (**E–H**). The formations of numerous autophagic vacuoles, including autophagosome with double-membrane structures and multilamellar bodies, were observed in the damaged cells on the injured side (**F–N**). A higher magnification of autophagosomes (arrows in **I, K, M**). The autophagosomes contained membranous structures and parts of the cytoplasm. A higher magnification of multilamellar bodies (arrowheads in **I, J, L, N**). Scale bars = 5 μm (**A, E, G**); 1 μm (**B, F, H**); and 250 nm (**C, D, I–N**).

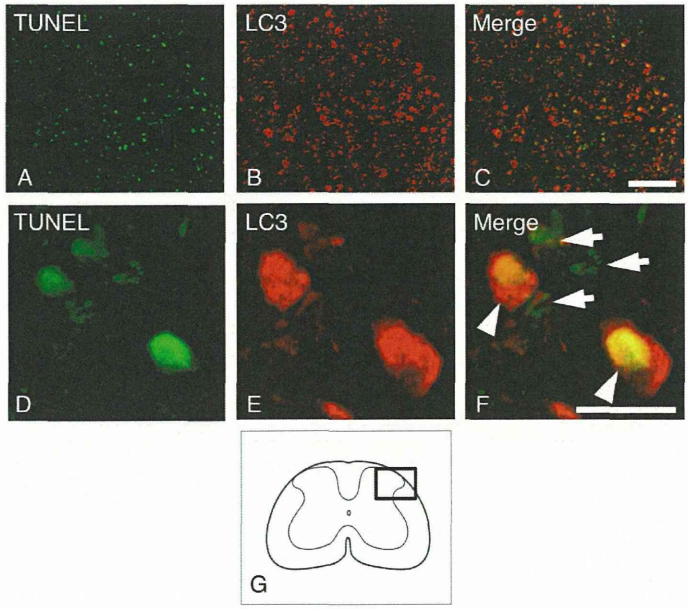

Figure 7. Double staining of LC3 (red) and TUNEL (green) on the injured side in transverse section at 3 days after hemisection (**A–F**). The LC3-positive cells were observed in TUNEL-positive cells. The nuclei in the TUNEL-positive cells showed that LC3 positive were round, which is consistent with autophagic cell death (arrowheads), and they were neither shrunken nor fragmented as is observed in apoptotic nuclei (arrows). Scale bars = 100 μm (upper panel) and 20 μm (lower panel). The schematic drawing illustrates the location of the micrographs (**G**).

in apoptotic nuclei. These results revealed both biochemically and anatomically that autophagy was clearly activated and autophagic cell death was induced in the damaged neural tissue after SCI.

An analysis of LC3 protein expression is the most used method to investigate the activity of autophagy.[20,21] The expression of LC3 increases at lesion sites after traumatic brain injury and cerebral ischemia.[16,22,25–27] These reports suggest that the autophagic activity increases in response to the neural tissue damage of brain. In this study, the immunohistochemical analysis showed that the number of LC3-positive cells significantly increased in the damaged neural tissue after SCI. Previous studies showed that the punctate LC3 dots in cytoplasm normally represent the LC3-II distribution located in autophagosomal membrane.[16,19] In our results, the LC3-positive cells in the injured spinal cord displayed numerous bright, punctate LC3 dots in cytoplasm. In addition, a Western blot analysis demonstrated that the level of LC3-II protein was significantly higher in the injured spinal cord than in the normal spinal cord. These results showed that the activity of

autophagy clearly increases at the lesion site after SCI as well as traumatic brain injury and cerebral ischemia.

Previous studies demonstrated the increased formation of autophagic vacuoles in many disease models using electron microscopy.[15,17] The formation of autophagic vacuoles increased in the damaged neural tissue after cerebral ischemia and traumatic brain injury.[22,24–27] These reports provided the morphologic evidence of the activation of autophagy in response to the neural tissue damage of brain. This study showed that the formation of autophagic vacuoles also increased in the damaged cells of the injured spinal cord. The current results anatomically demonstrated that autophagy was activated after SCI.

According to previous studies, at least three different types of cell death (necrosis, apoptosis, and autophagic cell death) are considered to participate in neural tissue damage.[16,32] Necrosis is morphologically characterized by swelling of the organelles and the cytoplasm, followed by the collapse of the plasma membrane and lysis of the cells.[33,34] Apoptosis is characterized by cellular shrinkage with condensation of the cytoplasm, sharply delineated of chromatin masses lying against the nuclear membrane, nuclear fragmentation, and the subsequent formation of membrane-confined apoptotic bodies. In addition, apoptosis is generally detected by using biochemical parameters, such as caspase activation, cytochrome *c* release, oligonucleosomal DNA fragmentation, and phosphatidylserine.[33,34] Autophagic cell death is morphologically distinct from apoptotic cell death. The increased formation of autophagic vacuoles is observed in autophagic cell death, but autophagic vaculoes are not induced in apoptosis.[13] The nucleus is shrunken and fragmented in apoptosis, but in autophagic cell death the nucleus does not change.[11,16,32] Previous studies have shown that autophagic cell death is induced in the damaged neural tissue after brain trauma and cerebral ischemia.[22,32] However, previous studies have focused on apoptotic process but not autophagic activity as mechanism of neural tissue damage after SCI. This study demonstrated that the formation of autophagic vacuoles obviously increased in damaged cells of the injured spinal cord under electron microscopy. Furthermore, most of the nuclei in the TUNEL-positive cells expressed LC3 were round, which is consistent with autophagic cell death, and they were neither shrunken nor fragmented as is observed in apoptotic nuclei. Therefore, on the basis of the anatomic formation of autophagic vacuoles, the increased expression of LC3 and the morphology of the nuclei in damaged cells, autophagic cell death should be induced in the lesion site after SCI.

Autophagy also affects the mechanism of apoptosis as well as autophagic cell death. The biochemical mechanisms of crosstalk between apoptosis and autophagy have been previously described.[5,35,36] Many recent studies have shown that autophagy and apoptosis share common regulatory elements including Bcl-2, DRAM, p53, and NFκB.[12,29] Previous research has demonstrated Beclin 1 to interact with Bcl-2, which is known as an antiapoptotic protein and contributes to the mechanism of apoptosis.[6] In our previous study, the Beclin 1 expression was upregulated after SCI.[28] In addition, the time course of the Beclin 1 expression was quite similar to that of apoptosis after SCI.[37–39] Furthermore, in this study, the LC3 expression was observed from 4 hours, peaked at 3 days, and continued to be observed for 21 days after SCI. The time course of the LC3 expression was also similar to that of both apoptosis and Beclin 1 expressin.[28,37–39] Therefore, these results suggested that autophagy could affect apoptotic process *via* Beclin 1 after SCI.

Previous studies showed that the autophagic activity increased in neurons after brain injury[25,26] and in astrocytes after oxidative injury.[40] The activation of autophagy is associated with demyelination in peripheral nerves in an experimental model of neuropathy in the rat.[41] These results suggested that autophagy contributed to the death of various cells and removed the damaged cells in response to the neural tissue injury. In this study, the expression of LC3 increased in neurons, astrocytes, and oligodendrocytes in the injured spinal cord. Therefore, the activity of autophagy increased in these cells and may contribute to the mechanism of neural cell loss after SCI.

Autophagy can be involved in not only cell death but also the cytoprotection.[5] Previous studies showed that autophagic cell death was induced in damaged neural tissue in focal cerebral ischemia and in closed head injury.[16,32] On the contrary, enhancing autophagy induced neuroprotection in traumatic brain injury and in neonatal brain hypoxia-ischemia induced injury.[6,42] This study revealed activation of autophagy and induction of autophagic cell death in the damaged neural tissue after SCI. However, whether the function of autophagy is protective or detrimental for neural tissue in SCI remains to be elucidated. Future studies are expected to further elucidate the molecular and biochemical mechanisms of autophagy in neural tissue damage after SCI.

CONCLUSION

The expression of LC3, a characteristic marker of autophagy, was significantly increased in the damaged neural tissue after SCI. In addition, the anatomic formation of autophagic vacuoles was obviously increased in the damaged cells. Furthermore, the nuclei in the TUNEL-positive cells showed that LC3 positive were round, which is consistent with autophagic cell death, and they were neither shrunken nor fragmented as observed in apoptotic nuclei. Thus, this study suggested both biochemically and anatomically that autophagy was clearly activated and autophagic cell death was induced at the lesion site in response to SCI.

➢ Key Points

- ❑ The expression of LC_3, a characteristic marker of autophagy, was significantly increased in the damaged neural tissue after SCI.
- ❑ The anatomic formation of autophagic vacuoles was obviously increased in the damaged cells. The nuclei in the TUNEL-positive cells that showed LC_3 positive were round, which is consistent with autophagic cell death.

❑ These results suggested both biochemically and anatomically that autophagy was clearly activated and autophagic cell death was induced at the lesion site after SCI.

Acknowledgments

We thank Dr. Koshi N. Kishimoto and Dr. Shigeyuki Tokunaga for useful discussion. We also thank Mr. Katsuyoshi Shoji, Ms. Sizue Mochizuki, Ms. Michiko Fukuyama, and Ms. Yukiko Sato for technical assistance, and Ms. Teruko Sueta and the animal care team at Institute for Animal Experimentation in Tohoku University for the animal care in this study.

References

1. Ogier-Denis E, Codogno P. Autophagy: a barrier or an adaptive response to cancer. *Biochim Biophys Acta* 2003;1603:113–28.
2. Gozuacik D, Kimchi A. Autophagy as a cell death and tumor suppressor mechanism. *Oncogene* 2004;23:2891–906.
3. Shintani T, Klionsky DJ. Autophagy in health and disease: a double-edged sword.*Science* 2004;306:990–5.
4. Rubinsztein DC, DiFiglia M, Heintz N, et al. Autophagy and its possible roles in nervous system diseases, damage and repair. *Autophagy* 2005;1:11–22.
5. Tsujimoto Y, Shimizu S. Another way to die: autophagic programmed cell death. *Cell Death Differ* 2005;12(suppl 2):1528–34.
6. Erlich S, Alexandrovich A, Shohami E, et al. Rapamycin is a neuroprotective treatment for traumatic brain injury. *Neurobiol Dis* 2007;26:86–93.
7. Hara T, Nakamura K, Matsui M, et al. Suppression of basal autophagy in neural cells causes neurodegenerative disease in mice. *Nature* 2006;441:885–9.
8. Komatsu M, Waguri S, Chiba T, et al. Loss of autophagy in the central nervous system causes neurodegeneration in mice. *Nature* 2006;441:880–4.
9. Pan T, Kondo S, Zhu W, et al. Neuroprotection of rapamycin in lactacystin-induced neurodegeneration *via* autophagy enhancement. *Neurobiol Dis* 2008;32:16–25.
10. Sarkar S, Ravikumar B, Floto RA, et al. Rapamycin and mTOR-independent autophagy inducers ameliorate toxicity of polyglutamine-expanded huntingtin and related proteinopathies. *Cell Death Differ* 2009;16:46–56.
11. Kitanaka C, Kuchino Y. Caspase-independent programmed cell death with necrotic morphology. *Cell Death Differ* 1999;6:508–15.
12. Scarlatti F, Granata R, Meijer AJ, et al. Does autophagy have a license to kill mammalian cells? *Cell Death Differ* 2009;16:12–20.
13. Clarke PG. Developmental cell death: morphological diversity and multiple mechanisms. *Anat Embryol (Berl)* 1990;181:195–213.
14. Larsen KE, Sulzer D. Autophagy in neurons: a review. *Histol Histopathol* 2002;17:897–908.
15. Matsui Y, Takagi H, Qu X, et al. Distinct roles of autophagy in the heart during ischemia and reperfusion: roles of AMP-activated protein kinase and Beclin 1 in mediating autophagy. *Circ Res* 2007;100:914–22.
16. Rami A, Langhagen A, Steiger S. Focal cerebral ischemia induces upregulation of Beclin 1 and autophagy-like cell death. *Neurobiol Dis* 2008;29:132–41.
17. Suzuki C, Isaka Y, Takabatake Y, et al. Participation of autophagy in renal ischemia/reperfusion injury. *Biochem Biophys Res Commun* 2008;368:100–6.
18. Ohsumi Y. Molecular dissection of autophagy: two ubiquitin-like systems. *Nat Rev Mol Cell Biol* 2001;2:211–16.
19. Kabeya Y, Mizushima N, Ueno T, et al. LC3, a mammalian homologue of yeast Apg8p, is localized in autophagosome membranes after processing. *EMBO J* 2000;19:5720–8.
20. Mizushima N. Methods for monitoring autophagy. *Int J Biochem Cell Biol* 2004;36:2491–502.
21. Klionsky DJ, Abeliovich H, Agostinis P, et al. Guidelines for the use and interpretation of assays for monitoring autophagy in higher eukaryotes. *Autophagy* 2008;4:151–75.
22. Adhami F, Liao G, Morozov YM, et al. Cerebral ischemia-hypoxia induces intravascular coagulation and autophagy. *Am J Pathol* 2006;169:566–83.
23. He Y, Wan S, Hua Y, et al. Autophagy after experimental intracerebral hemorrhage. *J Cereb Blood Flow Metab* 2008;28:897–905.
24. Lai Y, Hickey RW, Chen Y, et al. Autophagy is increased after traumatic brain injury in mice and is partially inhibited by the antioxidant gamma-glutamylcysteinyl ethyl ester. *J Cereb Blood Flow Metab* 2008;28:540–50.
25. Liu CL, Chen S, Dietrich D, et al. Changes in autophagy after traumatic brain injury. *J Cereb Blood Flow Metab* 2008;28:674–83.
26. Uchiyama Y, Koike M, Shibata M. Autophagic neuron death in neonatal brain ischemia/hypoxia. *Autophagy* 2008;4:404–8.
27. Wen YD, Sheng R, Zhang LS, et al. Neuronal injury in rat model of permanent focal cerebral ischemia is associated with activation of autophagic and lysosomal pathways. *Autophagy* 2008;4:762–9.
28. Kanno H, Ozawa H, Sekiguchi A, et al. Spinal cord injury induces upregulation of Beclin 1 and promotes autophagic cell death. *Neurobiol Dis* 2009;33:143–8.
29. Maiuri MC, Zalckvar E, Kimchi A, et al. Self-eating and self-killing: crosstalk between autophagy and apoptosis. *Nat Rev Mol Cell Biol* 2007;8:741–52.
30. Dong H, Fazzaro A, Xiang C, et al. Enhanced oligodendrocyte survival after spinal cord injury in Bax-deficient mice and mice with delayed Wallerian degeneration. *J Neurosci* 2003;23:8682–91.
31. Kalderon N, Fuks Z. Structural recovery in lesioned adult mammalian spinal cord by x-irradiation of the lesion site. *Proc Natl Acad Sci U S A* 1996;93:11179–84.
32. Diskin T, Tal-Or P, Erlich S, et al. Closed head injury induces upregulation of Beclin 1 at the cortical site of injury. *J Neurotrauma* 2005;22:750–62.
33. Krysko DV, Vanden Berghe T, Parthoens E, et al. Methods for distinguishing apoptotic from necrotic cells and measuring their clearance. *Methods Enzymol* 2008;442:307–41.
34. Krysko DV, Vanden Berghe T, D'Herde K, et al. Apoptosis and necrosis: detection, discrimination and phagocytosis. *Methods* 2008;44:205–21.
35. Boya P, González-Polo RA, Casares N, et al. Inhibition of macroautophagy triggers apoptosis. *Mol Cell Biol* 2005;25:1025–40.
36. Kanno H, Ozawa H, Sekiguchi A, et al. The role of autophagy in spinal cord injury. *Autophagy* 2009;5:390–2.
37. Citron BA, Arnold PM, Sebastian C, et al. Rapid upregulation of caspase-3 in rat spinal cord after injury: mRNA, protein, and cellular localization correlates with apoptotic cell death. *Exp Neurol* 2000;166:213–26.
38. Lu J, Ashwell KW, Waite P. Advances in secondary spinal cord injury: role of apoptosis. *Spine* 2000;25:1859–66.
39. Yong C, Arnold PM, Zoubine MN, et al. Apoptosis in cellular compartments of rat spinal cord after severe contusion injury. *J Neurotrauma* 1998;15:459–72.
40. Lee SJ, Cho KS, Koh JY. Oxidative injury triggers autophagy in astrocytes: the role of endogenous zinc. *Glia* 2009;57:1351–61.
41. Calle E, Berciano MT, Fernández R, et al. Activation of the autophagy, c-FOS and ubiquitin expression, and nucleolar alterations in Schwann cells precede demyelination in tellurium-induced neuropathy. *Acta Neuropathol* 1999;97:143–55.
42. Carloni S, Buonocore G, Balduini W. Protective role of autophagy in neonatal hypoxia-ischemia induced brain injury. *Neurobiol Dis* 2008;32:329–39.

Eur Spine J (2011) 20:1560–1566
DOI 10.1007/s00586-011-1724-7

ORIGINAL ARTICLE

Long-term results of double-door laminoplasty using hydroxyapatite spacers in patients with compressive cervical myelopathy

Atsushi Kimura · Atsushi Seichi · Hirokazu Inoue · Yuichi Hoshino

Received: 6 October 2010 / Revised: 24 January 2011 / Accepted: 6 February 2011 / Published online: 19 February 2011

Abstract No previous studies have reported 10-year follow-up results for double-door laminoplasty using hydroxyapatite (HA) spacers. The purpose of this study was therefore to explore the long-term results of double-door laminoplasty using HA spacers and to determine if non-union or breakage of HA spacers is related to restenosis of the enlarged cervical canal. The study group consisted of 68 patients with a minimum of 10 years of follow-up after double-door laminoplasty using HA spacers. The average postoperative Japanese Orthopaedic Association score improved significantly after surgery and was maintained until the final follow-up. The average range of motion decreased by 42.6% in patients with cervical spondylotic myelopathy (CSM) and 65.8% in patients with ossification of the posterior longitudinal ligament (OPLL). The enlarged cervical canal area was preserved almost until the final follow-up. The average non-union rates of HA spacers were 21% in CSM and 17% in OPLL, and the average breakage rates were 24 in CSM and 21% in OPLL at the final follow-up. Although non-union and breakage of HA spacers were common, neither of these factors were correlated with restenosis of the enlarged cervical canal.

Keywords Cervical myelopathy · Double-door laminoplasty · Hydroxyapatite spacer · Long-term outcome

A. Kimura (✉) · A. Seichi · H. Inoue · Y. Hoshino
Department of Orthopaedics, Jichi Medical University, 3311-1 Yakushiji, Shimotsuke, Tochigi 329-0498, Japan
e-mail: akimura@jichi.ac.jp

Introduction

Laminoplasty is a standard surgical option for the treatment of cervical myelopathy caused by multi-segmental cervical canal stenosis. Expansive open-door laminoplasty [1] and double-door laminoplasty [2] are two basic techniques used to enlarge a stenotic cervical canal, while preserving the posterior elements of the spine. Modifications of the various surgical techniques have included the use of hydroxyapatite (HA) spacers [3] or miniplates [4], the performance of an osteotomy using a thread-wire saw [5], and preservation of the muscular attachments to the spinous processes [6, 7]. The use of HA spacers instead of autologous bone grafts was developed to decrease the operative time and reduce blood loss and donor site morbidity [3].

There have only been a few long-term follow-up reports of open-door [1, 8, 9] and double-door laminoplasty [2], and these have focused on the use of autologous bone grafts [2, 9] or simple sutures [1, 8] to maintain an enlarged spinal canal; little is known regarding the long-term results of laminoplasty using HA spacers. In this study, we investigated the long-term outcomes over a 10-year follow-up period after double-door laminoplasty using HA spacers. We also investigated if non-union or breakage of the spacers was related to restenosis of the enlarged cervical canal.

Materials and methods

A total of 136 consecutive patients with compressive cervical myelopathy underwent double-door laminoplasty using HA spinous process spacers between 1995 and 1999. Of these 136 patients, 19 died of causes unrelated to

Table 1 Patient data

	CSM	OPLL
No. of patients	39	29
Male/female	24/15	21/8
Average age (years)	54.4 (35–77)	56.2 (35–71)
Average follow-up period (years)	12.4 (10–14)	12.7 (10–14)
Surgical levels		
C2–C7	23	22
C3–C7	11	1
C2–T1	5	4
C3–T1	0	2

CSM cervical spondylotic myelopathy, *OPLL* ossification of the posterior longitudinal ligament

cervical disease, 41 patients were lost to follow-up before completing the 10-year follow-up period, and 8 patients were excluded from the study because of hemiplegia due to brain infarction, concurrent anterior long fusion, or severe arteriosclerosis obliterans. The study group therefore included 68 patients who were followed for at least 10 years after surgery. The mean follow-up period was 12.2 years, ranging from 10 to 14 years. There were 39 patients with cervical spondylotic myelopathy (CSM) and 29 patients with ossification of the posterior longitudinal ligament (OPLL). The patients' demographic data are shown in Table 1. Age, sex, and preoperative clinical status did not differ significantly between the study population and the patients excluded from the study (data not shown).

The procedure for double-door laminoplasty has been described in detail elsewhere [2]. In most patients, the cervical laminae from C3 to C7 were exposed laterally to the medial aspect of the facet joints through a conventional midline approach. For a C2 split, the semispinalis cervicis, rectus capitis posterior major, and obliquus capitis inferior muscles were detached transiently. Bilateral gutters were made using a high-speed burr at the transitional area between the facet joint and the laminae, and the spinous processes were then split sagittally with a high-speed burr. The spinal canal was enlarged by opening the split laminae bilaterally with a spreader. To maintain the expanded position, HA spacers (Apacerum®; Asahi Optical Co., Ltd., Tokyo, Japan) were placed between the split laminae and fixed with nonabsorbable sutures. In the case of C2 laminoplasty, detached muscles were repaired with nonabsorbable sutures. Patients wore a cervical orthosis for approximately 2 weeks.

The clinical results were assessed using the Japanese Orthopaedic Association scoring system (JOA score) for treatment of cervical myelopathy. The JOA score consists of several categories of function, i.e., upper- and lower-limb motor function, sensory function, and bladder function. Surgical complications and prevalence of residual axial symptoms were investigated. The range of motion (ROM) between C2 and C7 was measured on flexion–extension radiographs taken before and 1, 2, 3, 5, and 10 years after surgery.

Twenty-seven of 68 patients (13 CSM patients and 14 OPLL patients) were examined using computed tomography (CT) before and after surgery (1 month, 1 year, and at the final follow-up). The transverse area of the cervical canal was measured at the level of the vertebral pedicles using computer software (Scion Image, Scion Corp, Frederick, MD) before and after surgery (1 month and at the final follow-up). Non-union between HA spacers and split spinous processes, and breakage of HA spacers, were evaluated by CT at 1 year after surgery and at the final follow-up. Non-union was defined as a clear zone detected between an HA spacer and the split spinous process (Fig. 5b), and breakage was defined as fracture of an HA spacer (Fig. 5c).

Data were analyzed statistically using SPSS for Windows (version 17.0, SPSS Inc., Chicago, IL). Unpaired *t* tests or Mann–Whitney *U* tests were used to detect differences between the two groups. A P value <0.05 was considered to be significant.

Results

The average JOA score improved significantly at 3 months after surgery and was maintained almost until the final follow-up in both the CSM and OPLL groups (Table 2). The time courses of the postoperative JOA scores for each category of function (upper- and lower-limb motor function, sensory function, and bladder function) are shown in Fig. 1. The average upper-limb motor and sensory scores increased significantly at 3 months after surgery and were both preserved until the final follow-up in both the CSM and OPLL groups. The lower-limb motor score also improved after surgery, but decreased after the third postoperative year. Twelve patients with CSM (31%) and 11 patients with OPLL (38%) showed declines in lower-limb motor scores of 1–2 points between 3 years after surgery and the final follow-up. Most of the patients who showed late deterioration in lower-limb function had complications that impaired ambulatory ability, such as osteoarthritis in the lower-limb joints (4 CSM patients and 2 OPLL patients), spinal canal stenosis at the thoracolumbar spine (3 CSM patients and 5 OPLL patients), degenerative disease of the brain (1 patient in each group), and arteriosclerosis obliterans (1 OPLL patient). In particular, spinal canal stenosis at the thoracolumbar spine was a major cause of reduction in lower-limb function in the OPLL group, and four patients required additional surgery of the

Table 2 Chronological changes in JOA scores after surgery

	JOA score			
	CSM	*P**	OPLL	*P**
Preoperative	11.0 ± 2.6		11.0 ± 2.5	
3 months after surgery	13.1 ± 1.8	0.0003	13.1 ± 1.7	0.0012
1 year after surgery	13.6 ± 2.1	<0.0001	13.8 ± 2.2	0.0002
3 years after surgery	13.6 ± 2.2	<0.0001	13.7 ± 2.0	0.0001
More than 10 years after surgery	13.1 ± 2.4	0.0008	13.0 ± 2.7	0.008

Values are mean ± SD

JOA Japanese Orthopaedic Association, *CSM* cervical spondylotic myelopathy, *OPLL* ossification of the posterior longitudinal ligament

* *P* by Mann–Whitney *U* test

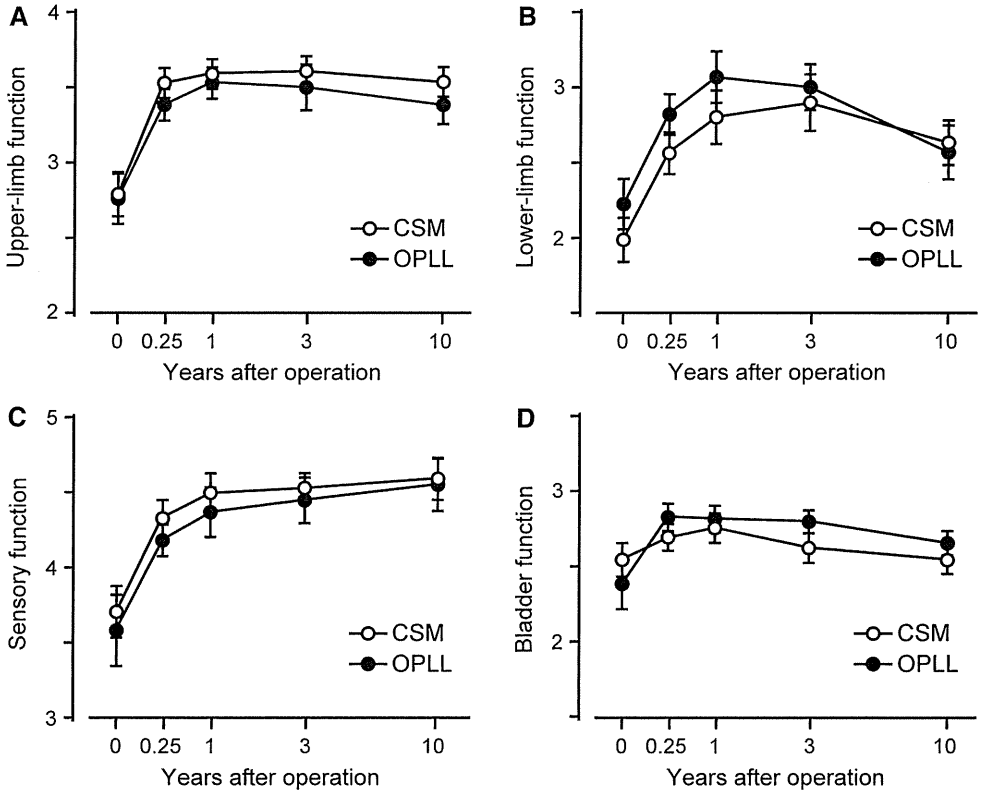

Fig. 1 Time-course of JOA score for each category of function. The average upper-limb motor and sensory scores improved significantly after surgery and were maintained almost until the final follow-up in both the CSM and OPLL groups. The lower-limb motor scores improved significantly, but gradually deteriorated after the third postoperative year in both groups. *Bars* indicate standard errors

thoracolumbar spine during the observation period. The average bladder function scores in both the CSM and OPLL groups increased after surgery, but had returned to preoperative levels at the final follow-up.

The most common postoperative complication was segmental motor weakness at the C5 segment, which developed in 4 (6%) out of 67 patients, although the symptoms resolved spontaneously within 1 year after surgery in all patients. Other complications included leakage of cerebrospinal fluid in three patients and transient deterioration of lower-limb function in one patient, all of which resolved without sequelae. One patient had lamina closure on the left side at C5 level due to fracture of a split spinous process. This patient had concomitant severe canal stenosis of the thoracic spine and showed impaired recovery of lower-limb function after surgery. He underwent simultaneous posterior thoracic spine decompression and a laminectomy at C5 at 6 months after the primary operation, which led to improved lower-limb function. Axial pain was one of the most common subjective symptoms during the follow-up period [6]. The percentage of patients with axial pain decreased over time, but 17 patients (25%) still complained of axial pain at the final follow-up.

The cervical ROM decreased over time and reached a plateau by 2 years after surgery (Fig. 2). The average ROMs in CSM and OPLL patients decreased from

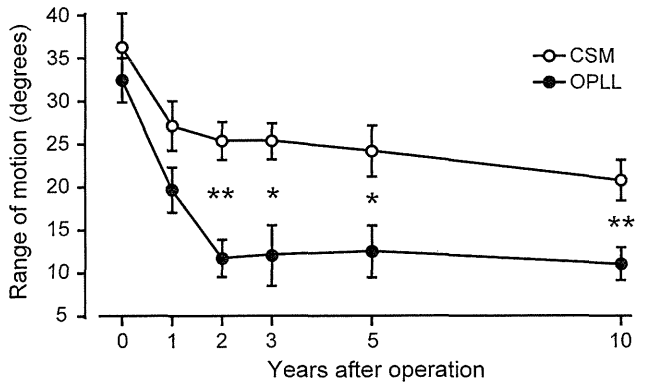

Fig. 2 Changes in cervical ROM. The cervical ROM decreased over time and reached a plateau by 2 years after surgery. The reduction in ROM was significantly larger in the OPLL group compared to the CSM group (66 vs. 43%, $P = 0.0052$) at the final follow-up. *Bars* indicate standard errors: $*P < 0.05$, $**P < 0.01$

preoperative values of 36.2° and 32.4° to postoperative values of 20.8° and 11.1°, respectively, at the final follow-up. The reduction in ROM was significantly larger in the OPLL group than in the CSM group (66 vs. 43%, $P = 0.0052$, 95% CI of the difference, 3.22–16.16). No patient in either group showed severe kyphotic deformity or instability at the final follow-up.

Chronological changes in cervical canal area, quantified by CT, are shown in Fig. 3. The average spinal canal area was significantly increased at every cervical level 1 month after surgery and was maintained almost until the final follow-up. The decrease in spinal canal area at the final follow-up was compared to that at 1 month after surgery to determine which cervical level was most susceptible to restenosis (Fig. 4). In patients with CSM, the decrease in canal area was smallest at the C3 level, while the canal area decreased preferentially in the upper cervical spine, with a maximum reduction of 9.9% at the C2 level, in OPLL patients.

The average rates of non-union between HA spacer and split spinous process were 27% in CSM and 25% in OPLL patients at 1 year after surgery (Table 3). The rates of non-union decreased over time, but remained at 21% in CSM and 17% in OPLL patients at the final follow-up. The average breakage rates of HA spacers in the CSM and OPLL groups were 8 and 4%, respectively, at 1 year after surgery, which increased to 24 and 21% at the final follow-up. However, all the bilateral gutters examined by CT demonstrated bone union by the final follow-up, and no spacers were significantly displaced from their original location. We also investigated the changes in spinal canal area between 1 month after surgery and the final follow-up to determine if non-union or breakage of HA spacers accelerated restenosis of the spinal canal. The percent changes in spinal canal area were comparable for both bony union and non-union in both the CSM and OPLL groups (Fig. 5d). In addition, no significant differences in the cervical canal area were detected for patients with intact HA spacers compared to those with broken HA spacers in either the CSM or OPLL groups (Fig. 5e).

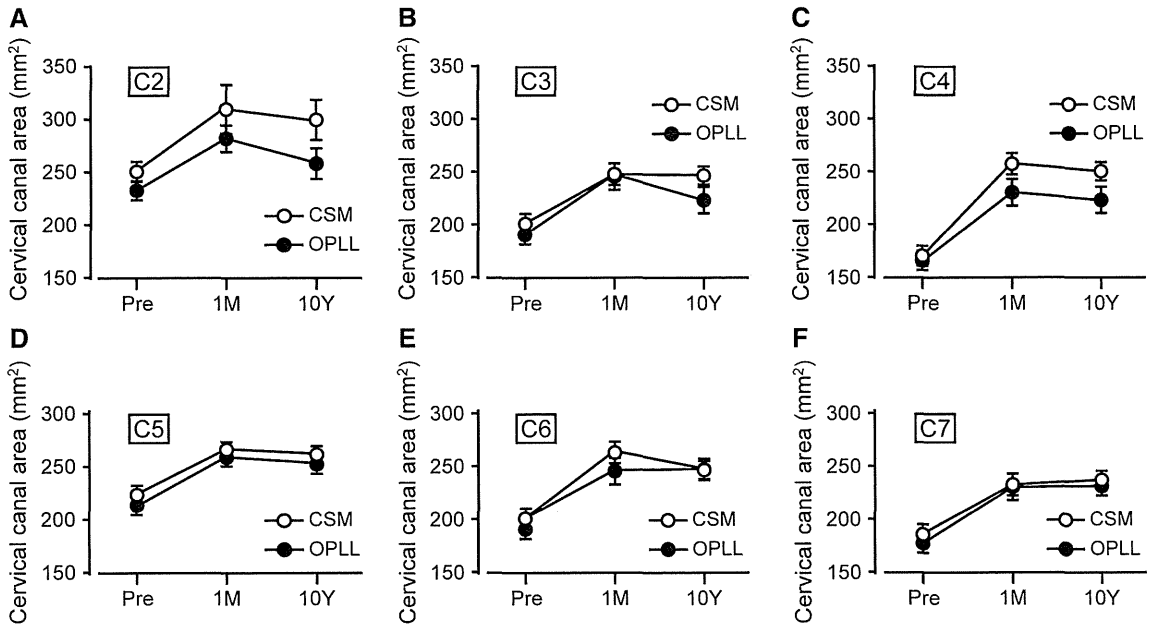

Fig. 3 Changes in spinal canal area quantified by CT. The average area of the spinal canal significantly increased at every cervical level 1 month after surgery and was maintained almost until the final follow-up (*Pre* preoperative, *1M* 1 month after surgery, *10Y* 10 years after surgery). *Bars* indicate standard errors

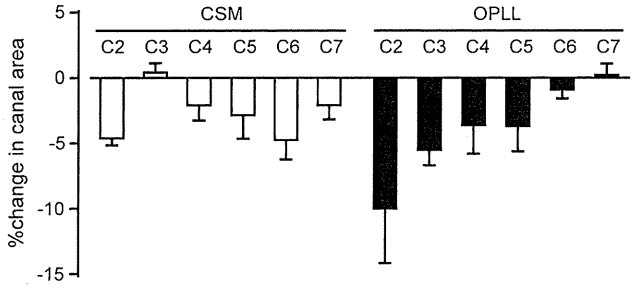

Fig. 4 Changes in cervical canal area at the final follow-up compared to 1 month after surgery. The decrease was smallest at the C3 level in patients with CSM. In patients with OPLL, the canal area decreased preferentially in the upper cervical spine, which showed a maximum reduction of 9.9% at the C2 level. *Bars* indicate standard errors

Discussion

The results of the current study demonstrated satisfactory long-term outcomes following double-door laminoplasty using HA spacers for compressive myelopathy. The average JOA score improved significantly at 3 months after surgery and was largely maintained during a minimum 10-year follow-up period in both CSM and OPLL patients. When the JOA score was divided into each functional category, the average score for lower-limb function gradually decreased over time, whereas upper-limb and sensory functions were stable during the observation period. The late deterioration of lower-limb function was largely attributable to degenerative changes, such as spinal canal stenosis at the thoracolumbar spine, osteoarthritis of the knee, and other general complications associated with aging. In particular, spinal canal stenosis at the thoracolumbar spine was the major cause of late deterioration of lower-limb function in patients with OPLL.

Several long-term studies of cervical laminoplasty found that the average ROM of the cervical spine substantially decreased over time [1, 2, 8, 9]. Seichi et al. [2] reported a 77% loss in the average ROM (36°–8°) over a 10-year follow-up of double-door laminoplasty using autologous bone grafts. Chiba et al. [1] reported that the pre- and postoperative ROMs were 44° and 14° in CSM and 32° and 11° in OPLL, respectively (a decrease of 68% in the CSM group and 66% in the OPLL group), over an average 14-year follow-up period after expansive open-door laminoplasty. The reductions in ROM in the current series (decreases of 43% in the CSM group and 66% in the OPLL

Table 3 Incidence of non-union and breakage of HA spacers

	No. of evaluated spacers	Non-union		Breakage	
		1 year	Final follow-up	1 year	Final follow-up
CSM ($n = 13$)	71	19 (27%)	15 (21%)	6 (8%)	17 (24%)
OPLL ($n = 14$)	77	19 (25%)	13 (17%)	3 (4%)	16 (21%)

HA hydroxyapatite, *CSM* cervical spondylotic myelopathy, *OPLL* ossification of the posterior longitudinal ligament

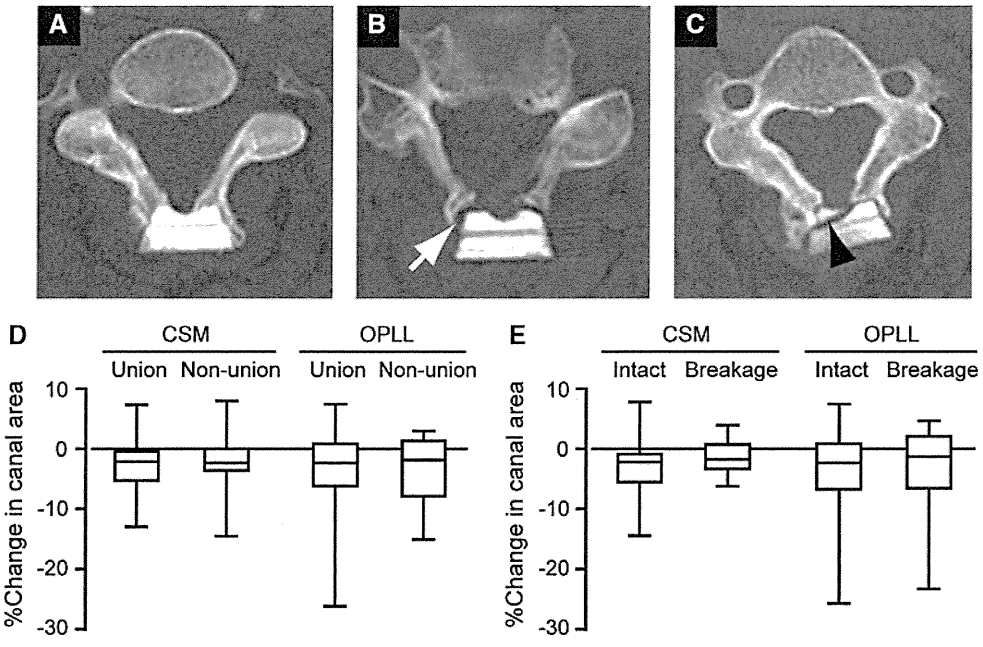

Fig. 5 Changes in cervical canal area in relation to the fate of HA spacers. Representative images of HA spacers with bone union (**a**), non-union (**b**), and breakage (**c**). Non-union was defined as a clear zone between the HA spacer and the split spinous process (*white arrow*), and breakage as fracture of an HA spacer (*black arrowhead*). *Box-and-whisker plots* demonstrate percent change in canal area. Neither non-union nor breakage of HA spacers correlated with restenosis of an enlarged cervical canal in either the CSM or OPLL groups (**d**, **e**)

group) were generally low, compared to these other long-term studies. The relative preservation of the ROM in the current study is attributable to the difference in the duration of cervical orthosis after surgery. Our patients wore a cervical orthosis for approximately 2 weeks, whereas patients in the previous studies wore an orthosis for 2–3 months after surgery. Several authors have proposed contracture of the paraspinal muscles and the facet joint as a potential cause of reduced cervical ROM after laminoplasty [7, 10, 11]. Early removal of the cervical orthosis and postoperative neck exercise are recommended to prevent atrophy and dysfunction of the paraspinal muscles. In addition, modified surgical techniques have been developed to preserve the paraspinal muscles, not only to maintain cervical ROM, but also to reduce axial symptoms [11, 12]. Roselli et al. [12] reported well-preserved cervical ROM after open-door laminoplasty using unilateral muscle dissection, while Takeuchi et al. [11, 13] maintained cervical ROM following double-door laminoplasty by preserving the semispinalis cervicis inserted into C2. Because bilateral muscle dissection is inevitable during double-door laminoplasty, further modifications to the surgical techniques are desirable to preserve the integrity of the cervical muscles.

One of the postoperative complications of cervical laminoplasty is restenosis of the enlarged spinal canal as a result of hinge closure [14]. One patient in our study required additional surgery because of hinge closure caused by fracture of the split spinous process. The constitutionally thin spinous process fractured spontaneously on the left side at the contact face with an HA spacer. This is a rare complication, but great care must be taken to avoid hinge closure resulting from fracture of a split spinous process. The incidences of other complications, such as segmental motor paresis, leakage of cerebrospinal fluid, and axial pain were similar to those demonstrated in long-term follow-ups of open-door laminoplasty [1, 9] and double-door laminoplasty using autologous bone grafts [2].

In this study, we focused on chronic changes in the cervical canal area over a 10-year period. The average cross-sectional area at each spinal level was significantly increased after surgery and was maintained almost until the final follow-up. The percent change in spinal canal area (comparison between the area at final follow-up and 1 month after surgery) revealed that the changes were smallest at the C3 spinal level in patients with CSM. This result may be related to the limited segmental motion between C2 and C3 caused by spontaneous lamina fusion, which occurs most commonly at the C2–C3 level [2]. The spinal canal area decreased preferentially in the upper cervical spine in patients with OPLL, especially at the C2 level. This can be attributed to the longitudinal growth of OPLL, which occurs preferentially in mixed and continuous types of OPLL after laminoplasty [8, 15]. Two patients showed obvious growth of the OPLL towards C2 and a mildly narrowed spinal canal in the upper cervical spine. However, neither of these patients showed deterioration of acquired function. The preserved function may have been attributed to restricted segmental motion in the upper cervical spine as a result of bridge formation by continuous type-OPLL.

Non-union and breakage of HA spacers at the final follow-up were not rare. However, none of the spacers were significantly displaced from their original location during the observation period. No patient in this study developed delayed dural damage or myelopathy due to displacement of HA spacers, as reported in other recent studies [16, 17]. Furthermore, neither non-union nor breakage of HA spacers correlated with restenosis of the enlarged spinal canal. These results suggest that rigid fusion between the HA spacer and the split spinous process is not essential for maintaining an enlarged spinal canal, even in the long-term. We speculate that HA spacers have fulfilled most of their roles by the time bone fusion has occurred in the lateral gutters, and that surgical techniques aimed at preventing the early displacement of HA spacers are essential for ensuring a good outcome after double-door laminoplasty. Kaito et al. [16] suggested that installing HA spacers at the base of the spinous process can help to prevent postoperative HA displacement. However, further prospective studies are needed to determine the most suitable surgical techniques.

This study had several limitations. It was a retrospective analysis involving a relatively small number of patients. In particular, limited CT data were available because of the retrospective nature of this study; however, functional outcomes estimated by JOA scores were comparable between patients who completed periodical CT scans and those who did not. Prospective controlled studies using patient-based outcomes are required to verify the efficacy of double-door laminoplasty using HA spacers.

Conclusions

The long-term results of double-door laminoplasty using HA spacers were satisfactory. Although non-union and breakage of HA spacers was not rare, an enlarged cervical canal was maintained over a 10-year period. Given the favorable long-term results with no donor site morbidity, the use of HA spacers for double-door laminoplasty is justified for the treatment of cervical myelopathy caused by multisegmental cervical canal stenosis. Further modifications of surgical technique are desirable to reduce postoperative complications, such as reduction in cervical ROM, segmental motor paresis, and axial symptoms.

Conflict of interest None.

References

1. Chiba K, Ogawa Y, Ishii K et al (2006) Long-term results of expansive open-door laminoplasty for cervical myelopathy—average 14-year follow-up study. Spine 31:2998–3005
2. Seichi A, Takeshita K, Ohishi I et al (2001) Long-term results of double-door laminoplasty for cervical stenotic myelopathy. Spine 26:479–487
3. Nakano K, Harata S, Suetsuna F et al (1992) Spinous process-splitting laminoplasty using hydroxyapatite spinous process spacer. Spine 17(Suppl 3):S41–S43
4. Tsuzuki N (1997) A novel technique for laminoplasty augmentation of spinal canal area using titanium miniplate stabilization: a computerized morphometric analysis. Spine 22:926–927
5. Martin-Benlloch JA, Maruenda-Paulino JI, Barra-Pla A et al (2003) Expansive laminoplasty as a method for managing cervical multilevel spondylotic myelopathy. Spine 28:680–684
6. Hosono N, Sakaura H, Mukai Y et al (2007) The source of axial pain after cervical laminoplasty—C7 is more crucial than deep extensor muscles. Spine 32:2985–2988
7. Kotani Y, Abumi K, Ito M et al (2009) Minimum 2-year outcome of cervical laminoplasty with deep extensor muscle-preserving approach: impact on cervical spine function and quality of life. Eur Spine J 18:663–671
8. Iwasaki M, Kawaguchi Y, Kimura T et al (2002) Long-term results of expansive laminoplasty for ossification of the posterior longitudinal ligament of the cervical spine: more than 10 years follow up. J Neurosurg 96(Suppl 2):180–189
9. Kawaguchi Y, Kanamori M, Ishihara H et al (2003) Minimum 10-year follow-up after en bloc cervical laminoplasty. Clin Orthop Relat Res 411:129–139
10. Iizuka H, Nakagawa Y, Shimegi A et al (2005) Clinical results after cervical laminoplasty: differences due to the duration of wearing a cervical collar. J Spinal Disord Tech 18:489–491
11. Takeuchi K, Yokoyama T, Ono A et al (2007) Cervical range of motion and alignment after laminoplasty preserving or reattaching the semispinalis cervicis inserted into axis. J Spinal Disord Tech 20:571–576
12. Roselli R, Pompucci A, Formica F et al (2000) Open-door laminoplasty for cervical stenotic myelopathy: surgical technique and neurophysiological monitoring. J Neurosurg 92:38–43
13. Takeuchi K, Yokoyama T, Ono A et al (2008) Limitation of activities of daily living accompanying reduced neck mobility after laminoplasty preserving or reattaching the semispinalis cervicis into axis. Eur Spine J 17:415–420
14. Yu HL, Xiang LB, Liu J et al (2010) Laminoplasty using Twinfix suture anchors to maintain cervical canal expansion. Eur Spine J 19:1795–1798
15. Hori T, Kawaguchi Y, Kimura T (2006) How does the ossification area of the posterior longitudinal ligament progress after cervical laminoplasty? Spine 31:2807–2812
16. Kaito T, Hosono N, Makino T et al (2009) Postoperative displacement of hydroxyapatite spacers implanted during double-door laminoplasty. J Neurosurg Spine 10:551–556
17. Kanemura A, Doita M, Iguchi T et al (2008) Delayed dural laceration by hydroxyapatite spacer causing tetraparesis following double-door laminoplasty. J Neurosurg Spine 8:121–128

Journal of Orthopaedic Surgery 2011;19(3):392-4

Ossification of the posterior atlantoaxial membrane associated with an os odontoideum: a case report

Junichi Ohya, Hirotaka Chikuda, Shurei Sugita, Takashi Ono, Yasushi Oshima, Katsushi Takeshita, Hiroshi Kawaguchi, Kozo Nakamura
Department of Orthopaedic Surgery, Faculty of Medicine, the University of Tokyo, Tokyo, Japan

ABSTRACT

We report a case of ossification of the posterior atlantoaxial membrane associated with an os odontoideum in a 46-year-old woman. She developed myelopathy following a minor motor vehicle accident. The patient underwent posterior atlantoaxial arthrodesis and resection of the ossified lesion and recovered uneventfully. Long-standing atlantoaxial instability might have played a role in ectopic ossification of the posterior atlantoaxial membrane.

Key words: *atlanto-axial joint; ligamentum flavum; ossification, heterotopic; spinal cord compression*

INTRODUCTION

The posterior atlantoaxial membrane is a collagenous tissue bridging the posterior arch of C1 and the cranial edge of the C2 lamina and acts as an additional stabiliser of the atlantoaxial complex.[1] Ectopic ossification of the membrane is rare and can cause severe myelopathy secondary to spinal cord compression. An os odontoideum is defined as an ossicle with smooth circumferential cortical margins and no osseous continuity with the body of axis.[2-4] Patients with an os odontoideum can present with pain or myelopathy, or remain asymptomatic. We report a patient with ossification of the posterior atlantoaxial membrane associated with an os odontoideum.

CASE REPORT

In June 2009, a 46-year-old woman presented with a one-month history of weakness in the upper extremities and gait disturbance and limited cervical motion following a minor motor vehicle accident. Neurological examination revealed weakness (grade 4/5) in her left deltoid, left biceps, left triceps, and bilateral intrinsic muscles. She had decreased sensation in the bilateral upper extremities, below the level of the C5 dermatome on the left and C7

Address correspondence and reprint requests to: Dr Hirotaka Chikuda, Department of Orthopaedic Surgery, Faculty of Medicine, the University of Tokyo, 7-3-1 Hongo, Bunkyo-ku, Tokyo, 113-8655, Japan. E-mail: chikuda-tky@umin.ac.jp

on the right. She also had intact cranial nerves and hyperreflexia on the left upper extremity with a positive Hoffmann sign; knee and ankle reflexes were increased bilaterally with positive Babinski signs. A spastic gait and clumsiness of her hands were evident, but there was no bowel or bladder difficulty.

Lateral radiographs showed an os odontoideum with atlantoaxial instability (Fig. 1). Reconstruction computed tomography demonstrated ossified tissue between the C1 posterior arch and the C2 lamina (Fig. 2). Magnetic resonance imaging demonstrated severe cord compression with intramedullary high signal intensity change (Fig. 3).

The patient underwent atlantoaxial stabilisation with transarticular screws. The dural sac was severely compressed by the ossified ligament even after anatomic reduction of the atlantoaxial joint. The posterior arch of C1 was then undercut for decompression, and the ossified lesion resected. Pathological examination of the specimen showed diffuse ossification in the degenerated ligament with irregular remodelling and hyperplasia of fibrous cartilage.

Immediately after surgery, motor weakness and sensory disturbance improved. At the 6-month follow-up, she had almost regained her full strength, and her gait disturbance had also been relieved. At month 12, she had returned to her job as a sports instructor. At month 18, she remained free of symptoms with solid bone fusion, despite having hyperreflexia in her lower extremities.

DISCUSSION

Ossification of the posterior atlantoaxial membrane is a rare cause of spinal cord compression. Only 5 such cases have been reported.[5–9] Most such patients were

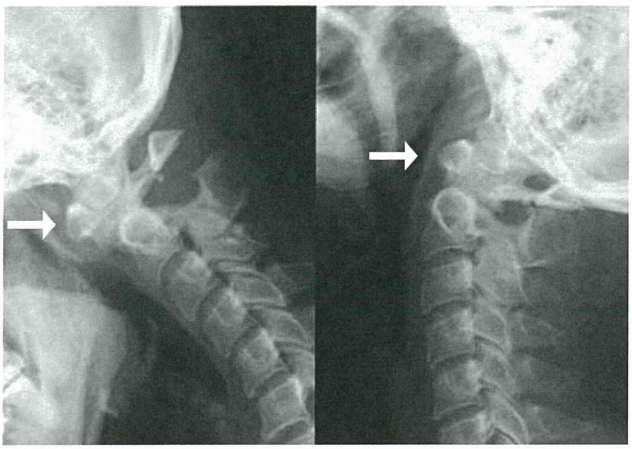

Figure 1 Flexion/extension lateral radiographs showing an os odontoideum (arrows) and atlantoaxial instability.

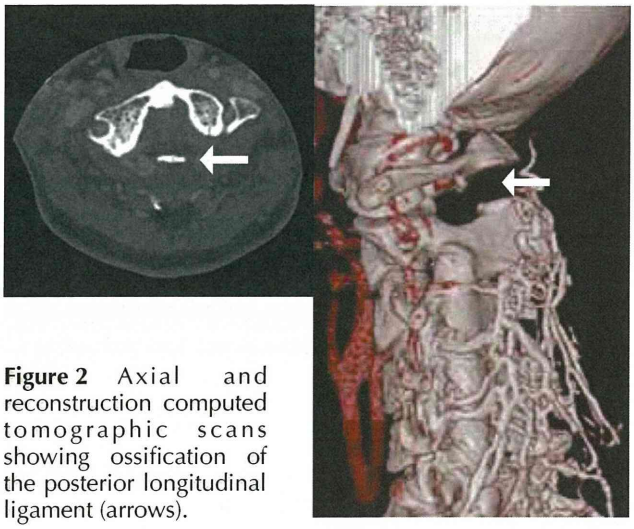

Figure 2 Axial and reconstruction computed tomographic scans showing ossification of the posterior longitudinal ligament (arrows).

Figure 3 T2-weighted magnetic resonance image demonstrating cord compression with intramedullary high signal intensity change.

Table
Patients with ossification of the posterior atlantoaxial membrane

Study[5–9]	Sex/age (years)	Type	C1-2 instability	Coexisting ossification	Surgery	Outcome
Yamaguchi et al,[5] 1992	M/46	Bilateral	-	No	Laminectomy	Improved
Kimura et al,[6] 1998	F/55	Unilateral	-	No	Laminectomy	-
Harimaya et al,[7] 2003	M/52	Bilateral	No	Anterior longitudinal ligament	Laminectomy	Improved
Nadkarni et al,[8] 2005	M/30	Bilateral	No	No	Laminectomy	Improved
Shoda et al,[9] 2005	M/70	Unilateral	No	Transverse ligament	Laminectomy	Improved
Present case	F/46	Tongue	Yes	No	Laminectomy, atlantoaxial stabilisation	Improved

in their fifth or sixth decade of life and presented with progressive myelopathy (Table). None but our patient showed atlantoaxial instability. Most of the ossified lesions showed laterality, as is often the case with the ossification of the ligamentum flavum in the thoracic spine.[10] Based on axial computed tomography, the condition can be classified as unilateral, bilateral, and tongue type (a flat lesion in the midline, as in our patient). The mainstay of treatment is laminectomy, and outcome is satisfactory for those without atlantoaxial instability.

The pathophysiological mechanism of this condition remains unclear. According to one theory, ossification of the ligamentum flavum often develops in the lower thoracic spine where the spine has more mobility than in the upper or middle thoracic regions. It is postulated that chronic mechanical stress on the ligament may lead to the development of the ossification.[11] Mechanical stress may induce osteogenic differentiation of the ligament cells.[12] In our patient, persistent atlantoaxial instability may have played a role in the ectopic ossification.

REFERENCES

1. Ramsey RH. The anatomy of the ligamenta flava. Clin Orthop Relat Res 1966;44:129–40.
2. Arvin B, Fournier-Gosselin MP, Fehlings MG. Os odontoideum: etiology and surgical management. Neurosurgery 2010;66(3 Suppl):S22–31.
3. Os odontoideum. Neurosurgery 2002;50(3 Suppl):S148–55.
4. Klimo P Jr, Kan P, Rao G, Apfelbaum R, Brockmeyer D. Os odontoideum: presentation, diagnosis, and treatment in a series of 78 patients. J Neurosurg Spine 2008;9:332–42.
5. Yamaguchi Y, Yamaguchi Y, Tokuhashi Y, Tomoyasu Y, Satoh K. Ossification of the atlanto-axial membrane: a case report [in Japanese]. Seikeigeka 1992;43:79–82.
6. Kimura S, Gomibuchi F, Ikezawa Y, Kaneko F, Uchiyama S, Homma T. Ossification of posterior atlantoaxial membrane. Case illustration. J Neurosurg 1998;89:491.
7. Harimaya K, Shiba K, Nomura H, Iwaki T, Takemitsu Y. Ossification of the posterior atlantoaxial membrane. Case report. J Neurosurg 2003;98(1 Suppl):S77–9.
8. Nadkarni TD, Menon RK, Desai KI, Goel A. Ossified ligamentum flavum of the atlantoaxial region. J Clin Neurosci 2005;12:486–9.
9. Shoda N, Anamizu Y, Yonezawa N, Ishibashi H, Yamamoto S. Ossification of the posterior atlantoaxial membrane and the transverse atlantal ligament. Spine (Phila Pa 1976) 2005;30:E248–50.
10. Kuh SU, Kim YS, Cho YE, Jin BH, Kim KS, Yoon YS, et al. Contributing factors affecting the prognosis surgical outcome for thoracic OLF. Eur Spine J 2006;15:485–91.
11. Matsumoto M, Chiba K, Toyama Y. Clinical manifestations of thoracic OPLL and OLF. In: Yonenobu K, Nakamura K, Toyama Y, editors. OPLL ossification of the posterior longitudinal ligament. 2nd ed. Tokyo: Springer; 2006:121–5.
12. Iwasaki K, Furukawa KI, Tanno M, Kusumi T, Ueyama K, Tanaka M, et al. Uni-axial cyclic stretch induces Cbfa1 expression in spinal ligament cells derived from patients with ossification of the posterior longitudinal ligament. Calcif Tissue Int 2004;74:448–57.

Spine

SPINE Volume 36, Number 9, pp E582–E587

CERVICAL SPINE

Risk Factors for Early Reconstruction Failure of Multilevel Cervical Corpectomy With Dynamic Plate Fixation

Atsushi Okawa, MD, PhD, Kenichiro Sakai, MD, PhD, Takashi Hirai, MD, Tsuyoshi Kato, MD, PhD, Shoji Tomizawa, MD, PhD, Mitsuhiro Enomoto, MD, PhD, Shigenori Kawabata, MD, PhD, Makoto Takahashi, MD, PhD, and Kenichi Shinomiya, MD, PhD

Study Design. Retrospective case series.

Objective. To investigate risk factors for early reconstruction failure of multilevel cervical corpectomy with dynamic plate fixation.

Summary of Background Data. For anterior cervical decompression and fusion, reinforcement by plate fixation was performed to decrease early reconstruction failure and to increase the fusion rate. However, a relatively high complication rate such as graft dislodgement, has been reported in patients undergoing multilevel corpectomy and reconstruction. Risk factors associated with early reconstruction failure have not been explicitly described.

Methods. In 30 instrumented multilevel corpectomy and reconstruction, medical records and radiographic studies were reviewed to investigate risk factors with regard to sagittal alignment of the cervical spine, graft subsidence, screws used in fixation, endplate preparation, and intermediate screw for fibular graft.

Results. Reconstruction failures included anterior slipping at the bottom of the graft in 2 cases, fracture of the C7 vertebral body in 2 cases, and pullout of a screw in 2 cases. Four patients were found to have nonunion of the graft at the final follow-up, but none had experienced early reconstruction failure.

On radiologic measurement, the fusion area lordotic angle after surgery in the patients with reconstruction failures was significantly larger than that of the patients with no complications. The postoperative C2–C7 lordotic angles of the patients with reconstruction failure were also larger, but this trend was not statistically significant. No other factor, such as age and gender, type of screw used, intermediate screw or preservation of the endplates was related to reconstruction failures in this study.

Conclusion. Postoperative cervical hyperlordosis may adversely affect graft stability in the early postoperative period of the surgery of corpectomy and reconstruction with dynamic plate fixation.

Key words: anterior cervical fusion, anterior cervical plate, complication, cervical myelopathy, ossification of longitudinal ligament. **Spine 2011;36:E582–E587**

Corpectomy and reconstruction are the treatment of choice in patients with ossification of the posterior longitudinal ligament (OPLL) or spondylotic myelopathy with a kyphotic alignment of the cervical spine. We have previously reported that the anterior floating method appears to yield adequate long-term outcomes when used to treat OPLL.[1] However, a relatively high complication rate, which includes complications such as respiratory distress and graft dislodgement, has been reported in patients undergoing multilevel corpectomy and reconstruction. Previous studies have found that graft reinforcement with anterior plate fixation is expected to decrease early reconstruction failure and to increase the fusion rate in patients undergoing multilevel corpectomy.[2,3]

However, Sasso *et al* reported a 71% failure rate after 3-level fixed plated reconstruction.[4] Daubs also reported an extremely high early failure rate (75%) with the use of a titanium mesh cage and a fixed anterior plate for reconstruction in patients undergoing multilevel corpectomies.[5] Interestingly, in a biomechanical experiment, Brodke *et al* found that a static plate loses its loadsharing capacity after 10% subsidence has occurred.[6] In contrast, with regard to the choice of the type of fixation that is used (*i.e.*, a constrained *vs.* a semiconstrained plate), most recent studies have reported that dynamic plate designs provide a faster fusion of the cervical spine in comparison to rigid plate designs.[7–10] In these reports, however, the authors did not include a detailed discussion of the complications associated with early reconstruction failure in multilevel corpectomy.[11]

This article details the results of a retrospective study of the factors associated with early reconstruction failure in patients undergoing multilevel corpectomy with dynamic plate fixation. Specifically, we review the preoperative and postoperative

From the Department of Orthopedic and Spinal Surgery, Graduate School of Medicine, Tokyo Medical and Dental University, Tokyo, Japan.

Acknowledgment date: October 28, 2009. First revision date: February 12, 2010. Second revision date: March 12, 2010. Acceptance date: March 12, 2010.

The device(s)/drug(s) is/are FDA-approved or approved by corresponding national agency for this indication.

No funds were received in support of this work. No benefits in any form have been or will be received from a commercial party related directly or indirectly to the subject of this manuscript.

Address correspondence and reprint requests to Atsushi Okawa, MD, PhD, Department of Orthopedic and Spinal Surgery, Tokyo Medical and Dental University, Yushima 1–5-45, Bunkyo-Ku, Tokyo 113– 8519, Japan; E-mail: okawa.orth@tmd.ac.jp

DOI: 10.1097/BRS.0b013e3181e0f06a

sagittal alignment of the cervical spine, the screws used in fixation, the use (or lack of use) of an intermediate screw for fibula grafts, the methods that were used for endplate preparation, and the characteristics of patients who required repeat surgery in the early postoperative period.

MATERIALS AND METHODS

Materials

Between 2000 and 2008, 31 patients with myelopathy caused by multilevel cervical spondylosis (n = 7) or OPLL (n = 24) underwent multilevel corpectomy and reconstruction with autologous fibula and anterior cervical plate placement. One patient with spondylotic amyotrophy was included in the group of patients with cervical spondylosis. Our patients were divided into 2 groups based on the operative methods we used: long fusion (LF) was defined as multilevel corpectomy and reconstruction without segmental fusion, and a hybrid group (HF) was defined as a combination of segmental fusion and multilevel corpectomy and reconstruction (Table 1). One patient treated with LF was lost to follow-up after within 1 year of surgery. Therefore, a total of 30 patients (3 female, 27 male) were observed for a minimum of 1 year after surgery. The average follow-up period was 3.5 years in this patient population. When we define a disc-level as "1 segment," we performed 3-segment (n = 14), 4-segment (n = 13), and 5-segement fusion (n = 3). In the LF group, there were 14 cases of 2-level corpectomy and reconstruction, 10 cases of 3-level corpectomy and reconstruction, and 1 case of 4-level corpectomy and reconstruction. In the HF group, there were 3 cases of 4-segment fusion (a discectomy and 2-level corpectomy), and 2 cases of 5-segment fusion (1- or 2-level discectomy and 3- or 2-level corpectomy, respectively).

Clinical results were evaluated using the Japanese Orthopedic Association (JOA) scoring system for cervical myelopathy, and the JOA score recovery rate was calculated using Hirabayashi's method.[1]

The surgical procedure we used consisted of a standard anterior approach to the cervical spine with intraoperative spinal cord monitoring using motor-evoked potentials while the patient was under general anesthesia. No traction was used during the procedure. Lordosis of the cervical spine was maintained with a contoured foam pillow that was placed beneath the neck during the operation. Osteophytes that were compressing the spinal cord were removed using the microscope, and ossification of the posterior ligament was treated using an air drill such that the ligament was thinned and was allowed to migrate anteriorly (this is known as the "floating" method).[1,12] The endplates of the adjacent vertebral bodies were retained whenever possible but were sometimes removed to decompress areas of ossification behind the vertebral body or to better fit the vertebral column to the shape of the graft.

For reconstruction, a fibular bone graft reinforced by a rotationally dynamic plate was typically used. We used a fixedtype screw for the bottom and a variable-type screw for the top of the graft. This configuration allows the screws to pivot while preventing screw pullout.[7] A fibular bone graft reinforced by an anterior plate was used in 30 cases, and in 18 of these cases intermediate screws were added. The length and shape of the grafts were chosen such that the decompressed cervical column was extended slightly by mild manual distraction or with a Casper distractor.

The average operation time was 6 hours 3 minutes and ranged from 3 hours 25 minutes to 9 hours 15 minutes. The mean estimated blood loss during the operation was 440 mL (range: 70–2885 mL). Patients were permitted to walk 2 to 5 days after surgery and were placed in Philadelphia-type collars for 3 months. The length of admission ranged from 15 to 79 days (mean: 29 days). Patients' JOA scores before the operation ranged from 6 to 14.5 points with a mean of 11.0 ± 2.6 points. The JOA scores at the final follow-up appointment were 14.7 ± 2.3 points in the LF group and 14.9 ± 1.7 points in the HF group. The recovery rates of the JOA scores were 64.8% ± 27.9% in the LF group and 58.5% ± 50.5% in the HF group. Clinical outcomes did not differ significantly between the groups. Three patients experienced neurologic complications; 2 developed C5 palsy and 1 developed myelopathy (Table 2). One of the patients with C5 palsy also showed evidence of graft migration and screw pullout. All of the patients with neurologic complications had repeat surgery within 1 week after the initial surgery and had regained normal function by their 1-year follow-up appointment. Two of these patients displayed evidence

TABLE 1. Characteristics of 30 Patients

Median age (range)	59 (44–79)
Gender (male:female)	27:3
Segments fused (cases)	
3	14
4	13
5	3
Type of fusion (fibula: hydroxyapatite)	
Long (LF)	25
Hybrid (HF)	5

LF indicates multilevel corpectomy and fusion; HF, a combination of segmental fusion and multilevel corpectomy with fusion.

TABLE 2. Complication

Neurological deterioration	
C5 palsy	2
Myelopathy	1
Reconstruction failure	
Graft migration	2*
C7 body fracture	2*
Screw pullout	2 (4)†

**One of the patients with graft migration and one of the patients with a C7 fracture had screws that had dislodged.*

†Two patients showed only dislodged screws; this event coincided with graft migration and C7 fracture in other 2 patients.

of nonunion of the graft at their final follow-up appointment, which was most likely due to the fact that the graft was shortened somewhat during the second operation for neurologic complication. An additional 2 patients who had no particular risk factors also displayed evidence of nonunion at their 1-year follow-up appointments.

The clinical outcomes of these patients were not statistically significantly inferior to those of the patients who did not experience nonunion, but none of these 4 patients did exhibit early reconstruction failure.

Methods

This study is a case series of 30 patients who underwent multilevel corpectomy and reconstruction. Their medical records and radiographic studies were reviewed to investigate their individual risk factors for reconstruction failure.

We defined early reconstruction failure as graft migration, vertebral body fracture, or screw extrusion within 1 month of the index surgery regardless of whether it required repeat surgery. We examined the patients' surgical records to collect data regarding the type of screws that were used as well as whether the endplates were preserved. A series of lateral plain radiographs of the cervical spine were obtained to identify the presence of any implant or graft movement as well as to evaluate fusion status. Postoperative radiologic evaluation was performed on the radiographs that were taken within 1 week of surgery on the first day that patients were allowed to ambulate. Graft subsidence was defined as a >2 mm graft sinkage and was assessed by comparing lateral radiographs taken at 1 week and 1 month after the surgery. When either abnormal graft movement or screw pullout was suspected, a computer-assisted tomography (CT) scan was performed. This approach allowed us to detect fine fracture lines and anterior slippage at the bottom of the graft. Reformatted CT views that were obtained just after the surgery were also used for radiologic measurements when the borders of the C7 vertebral body were not clearly visible.

Sagittal alignment of the cervical spine was evaluated by measuring the C2–C7 angle between the tangential lines drawn from the posterior border of the C2 and C7 vertebral bodies. The lordotic angle of the fusion area was determined in a similar manner. The C7 horizontal angle was defined as the upper endplate angle of the C7 vertebral body viewed from the horizontal plane of the neutral lateral view. This angle was assessed with a radiograph that was taken with the patient in a sitting position. The graft was determined to have fused if there was absence of motion of the adjacent vertebral bodies and spinous processes in flexion-extension radiographs. We used the χ^2 test and Student's unpaired t test for our statistical analyses. All $P < 0.05$ were considered to be statistically significant.

RESULTS

The causes of reconstruction failures for which the patients underwent secondary operations included graft migration (n = 2), fracture of the C7 vertebral body (n = 2), and screw pullout (n = 2) (Table 2). Because one of the patients who experienced graft migration and one of the patients who experienced a C7 fracture also presented with screw pullout, a total of 4 patients had screws that had protruded. Four patients who had experienced graft migration or C7 fracture were treated by posterior spinous process wiring. Two patients with screw pullout had their implants removed after fusion was completed.

Reconstruction failures were observed in 5 patients in the LF group and in 1 patient in the HF group. A total of 1 of 14 patients who underwent 3-segment fusion, 3 of 13 patients who underwent 4-segment fusion, and 2 of 3 patients who underwent 5-segment fusion eventually presented with reconstruction failures. The number of segments that were fused was found to be statistically significantly related to the risk of reconstruction failures ($P < 0.05$). The following factors were not associated with reconstruction failure; nor with age, gender, the preservation of the vertebral endplates, screw type, the occurrence of postoperative graft subsidence within 1 month of surgery, and the use of intermediate screws for fibular grafting (Table 3).

With regard to radiologic measurements, the mean preoperative C2–C7 lordotic angle of patients who experienced reconstruction failure was 13.5° ± 10.9°, and that of the patients who did not experience any complications was 13.5° ± 17.1°. The fusion area lordotic angle of the patients who experienced reconstruction failure was 9.6° ± 13.1°, and that of the patients who did not experience complications was 7.4° ± 9.1°. There were no significant differences observed between the preoperative C2–C7 lordotic angles or the fusion area lordotic angles of these 2 groups.

The postoperative C2–C7 lordotic angle of the patients who experienced reconstruction failures tended to be larger than those of patients who did not experience reconstruction failure, but this trend was not significant. The fusion area lordotic angle of the patients who experienced reconstruction failure was 15.6° ± 8.4°, which was significantly ($P < 0.05$) larger than that of the patients who did not experience reconstruction failure (8.6° ± 6.4°)

TABLE 3. Factors Related to Reconstruction Failures

	Reconstruction Failures (6)	No Complication (24)	*P*
Average number of fused segments	4.2	3.5	$P < 0.05$
Removal of the top endplate of the fused area	4	6	$P < 0.1$
Removal of the bottom endplate of the fused area	4	13	n.s.
Fixed screw used at both ends	1	4*	n.s.
Intermediate screw	3/6	15/24†	n.s.
Subsidence	3	12	n.s

**No documentation about the screw in the 2 operative records.*
†Excluding HA graft.